

Evaluating the performance of a Picarro G2207-*i* analyser for high-precision atmospheric O₂ measurements

Leigh S. Fleming^{1,2}, Andrew C. Manning¹, Penelope A. Pickers¹, Grant L. Forster^{1,3,2}, and Alex J. Etchells¹

5 ¹Centre for Ocean and Atmospheric Sciences, School of Environmental Sciences, University of East Anglia, Norwich, UK

²Now at: GNS Science, Gracefield, Lower Hutt, 5040, New Zealand

³National Centre for Atmospheric Science, University of East Anglia, UK

Correspondence to: Leigh Fleming (l.fleming@gns.cri.nzleigh.fleming@uea.ac.uk)

Abstract.

10 Fluxes of oxygen (O₂) and carbon dioxide (CO₂) in and out of the atmosphere are strongly coupled for terrestrial biospheric exchange processes and fossil fuel combustion but are uncoupled for oceanic air-sea gas exchange. High-precision measurements of both species can therefore provide constraints on the carbon cycle and can be used to quantify fossil fuel CO₂ (ffCO₂) emission estimates. In the case of O₂, however, due to its large atmospheric mole fraction ~~of O₂~~ (~20.9 %) it is very challenging to measure small variations to the degree of precision and accuracy required for these applications. We have tested 15 an atmospheric O₂ analyser based on the principle of cavity ring-down spectroscopy (Picarro Inc., model G2207-*i*), both in the laboratory and at the Weybourne Atmospheric Observatory (WAO) field station in the UK, in comparisons to well-established, pre-existing atmospheric O₂ and CO₂ measurement systems.

In laboratory tests analysing ~~dry~~ air in high-pressure cylinders, ~~from the Allan deviation we found that the best precision was achieved with 30 minute averaging and was improved to ± 0.5 ppm ($\sim \pm 2.4$ per meg), after 30 minute averaging calculated a precision of ± 1 ppm (1 standard deviation of 300 seconds mean), and also from continuous measurements from a cylinder of dry air, we found the~~ 20 24-hour peak-to-peak range of hourly averaged values ~~of to be~~ 1.2 ppm (~ 5.876 per meg). These results are close to atmospheric O₂ compatibility goals as set by the UN World Meteorological Organization. ~~FB~~ But from measurements of ambient air conducted at WAO we found that the built-in water correction of the G2207-*i* does not sufficiently correct for the influence of water vapour on the O₂ mole fraction. When sample air was ~~pre~~-dried and ~~employing~~ a 5-hourly 25 baseline correction with a reference gas cylinder ~~was employed~~, the G2207-*i*'s results showed an average difference from the established O₂ analyser of 13.6 ± 7.5 per meg (over two weeks of continuous measurements). Over the same period, based on measurements of a so-called "target tank" (~~sometimes known as a "surveillance tank"~~), analysed for 12 minutes every 7 hours, we calculated a repeatability of $\pm 5.7 \pm 5.6$ per meg and a compatibility of $\pm 10.0 \pm 6.7$ per meg for the G2207-*i*. To further examine the G2207-*i*'s performance in real-world applications we used ambient air measurements of O₂ together with 30 concurrent CO₂ measurements to calculate ffCO₂. Due to the imprecision of the G2207-*i*, the ffCO₂ calculated showed large differences from that calculated from the established ~~measurement~~ system, and had a large uncertainty of ± 13.0 ppm, which was roughly double that from the established system (± 5.8 ppm).

1 Introduction

Oxygen (O_2) is the most abundant molecule in the atmosphere after nitrogen (N_2), with an atmospheric background mole fraction of approximately 20.94 % (Tohjima et al., 2005). Due to this large atmospheric background, O_2 measurements are sensitive to [changes-variations](#) in the mole fractions of [trace gases other atmospheric species](#), such as carbon dioxide (CO_2), [due to dilution effects](#). O_2 measurements are therefore typically reported on a relative scale calculated as the change in the ratio of O_2 to N_2 relative to a standard O_2/N_2 ratio, as given in Eq. (1), and expressed in “per meg” units.

$$\delta \left(\frac{O_2}{N_2} \right) = \left(\frac{O_2/N_2 \text{ sample} - O_2/N_2 \text{ reference}}{O_2/N_2 \text{ reference}} \right) \times 10^6 \quad (1)$$

In practice, atmospheric N_2 is far less variable than O_2 meaning that changes in the O_2/N_2 ratios can be assumed to be representative of O_2 mole fraction (Keeling and Shertz, 1992). In comparing changes in O_2 to changes in CO_2 , on a mole for mole basis, a 1 per meg change in O_2 is equivalent to a 0.2094 ppm (parts per million) change in CO_2 mole fraction (Keeling et al., 1998).

Over the past three decades atmospheric O_2 has been decreasing at [an average](#) rate of ~ 15 per meg yr^{-1} , primarily owing to fossil fuel combustion (Keeling and Manning, 2014); [over the same period, atmospheric \$CO_2\$ has been increasing at an average rate of 2 ppm \$yr^{-1}\$](#) . [In contrast the atmospheric \$CO_2\$ mole fraction has increased from approximately 277 ppm at the beginning of the industrial era to 4120 ppm in 2019–2020](#) (Dlugokenky and Tans, 2022), also predominantly due to fossil fuel combustion. For most processes that cause variability in atmospheric O_2 , there is an anti-correlated change in atmospheric CO_2 , therefore high-precision measurements of atmospheric O_2 play an increasingly important role in our understanding of atmospheric CO_2 , carbon cycling, and other biogeochemical processes (e.g. Pickers et al., 2017; Resplandy et al., 2019; Battle et al., 2019; Tohjima et al., 2019). Fluxes of O_2 and CO_2 in and out of the atmosphere are strongly coupled for terrestrial biosphere exchange with a global average oxidative ratio (OR) in the range of 1.03 to 1.10 $mol \text{ mol}^{-1}$ (Severinghaus, 1995). For fossil fuel combustion, dependent on fuel type, the OR is in the range of 1.17 to 1.95 $mol \text{ mol}^{-1}$ (Keeling, 1988a). Whereas O_2 and CO_2 fluxes are uncoupled for oceanic air-sea gas exchange primarily due to inorganic reactions in the water involving the carbonate system and not O_2 , as well as differences in air-sea equilibration times between the two gases.

The relationship between O_2 and CO_2 fluxes has also allowed for the derivation of the tracer “[aAtmospheric \$p\$ Potential \$e\$ Oxygen](#)” (APO), as defined in Eq. (42) (Stephens et al., 1998).

$$APO \approx O_2 + (-1.1 \times CO_2) \quad (2)$$

Where the factor -1.1 represents the mean value of the $O_2:CO_2$ OR for terrestrial biosphere photosynthesis and respiration (Severinghaus, 1995), [and where we have ignored very minor influences from methane and carbon monoxide](#). APO is therefore, by definition, invariant with respect to the terrestrial biosphere. Changes in APO therefore mainly reflect changes in ocean-atmosphere exchange of O_2 and CO_2 (primarily on seasonal and longer timescales), with a contribution from fossil fuels on both shorter and longer timescales. APO can thus be used to examine oceanic CO_2 fluxes and to quantify fossil fuel CO_2 (ff CO_2) emissions (Pickers et al., 2022).

65 The World Meteorological Organization (WMO) Global Atmosphere Watch (GAW) programme has established a measurement compatibility goal for O₂ of ± 2 per meg (± 0.4 ppm) (Crotwell et al., 2019), where compatibility refers to the acceptable level of agreement between two field stations or laboratories when measuring the same air sample. ~~This~~ is the scientifically desirable level of compatibility required to resolve, for example, latitudinal gradients and long-term trends (Crotwell et al., 2019). There is also a WMO extended compatibility goal of ± 10 per meg (± 2 ppm) which is suitable for

70 some specific applications when expected variations are relatively large (Crotwell et al., 2019), such as fossil fuel quantification in large cities. In order to be able to meet the WMO compatibility goals, it is recommended that a measurement system's repeatability and analytical precision should not exceed half of the compatibility goal (i.e., ± 1 per meg, ± 0.2 ppm). ~~Where the r~~Repeatability refers to the closeness of agreements between results of measurements of the same measure (which can also be defined sometimes referred to as the measurement system's precision). However, routinely achieving a

75 measurement precision repeatability of ± 1 per meg, is not yet achievable for the majority of almost any laboratories and/or field stations making high-precision measurements of atmospheric O₂. The large atmospheric background of O₂ makes it extremely challenging to measure the relatively small variations to the level of precision repeatability required, since measuring a change of 0.2 ppm against the background (~209400 ppm) requires a relative precision-repeatability of 0.0001 %.

Presently, there are several different analytical techniques available for measuring atmospheric O₂ to a high precision:

80 interferometry (Keeling, 1988b), isotope ratio mass spectrometry (Bender et al., 1994), paramagnetic techniques (Manning et al., 1999), vacuum ultraviolet absorption (VUV) (Stephens et al., 2011), gas chromatography (Tohjima, 2000), and electrochemical fuel cells (Stephens et al., 2007). The most precise of these current methods is the VUV absorption technique however, VUV O₂ analysers are "homemade" and are not commercially available thus limiting their widespread applications.

85 None of these techniques are "off-the-shelf" instruments systems, all of them are complex and time-consuming systems to design, build, and optimise, with very precise pressure, temperature, and flow control needed. All of the techniques also require frequent interruption to sample measurement to carry out calibration procedures (Kozlova and Manning, 2009). The supply of calibration gases for such systems is particularly labour intensive, both due to their relatively rapid consumption rate and that no commercial gas supply company is able to provide suitable gas mixtures for atmospheric O₂ research. Accurate, high-precision atmospheric O₂ measurements therefore remain challenging. An alternative commercially available O₂ analyser with

90 less requirements for external gas handling, air-sample drying, and calibration procedures could consequently revolutionise the field of atmospheric O₂ measurements if the required performance could be achieved and if it were relatively easy to operate with low maintenance requirements and a lower rate of calibration gas consumption.

In this paper we present the results from the analysis of a Picarro Inc. G2207-i Oxygen analyser, which operates on the principle of cavity ring-down spectroscopy technology (CRDS) (hereafter referred to as the G2207-i) and evaluate its performance in

95 comparison to established O₂ measurement systems in the University of East Anglia (UEA) Carbon Related Atmospheric Measurements (CRAM) Laboratory and at the Weybourne Atmospheric Observatory (WAO; North Norfolk, UK). Unlike most other analytical techniques used for atmospheric O₂ measurements, it is intended that the G2207-i does not require a continuous reference gas supply, it has built-in pressure and flow control, and it has the potential for much reduced sample

dry requirements due to a built-in water measurement and correction procedure. These features make the G2207-*i* a 100 potentially desirable analyser for high-precision atmospheric O₂ research, but we note that it would still require the same rigorous calibration procedures as other analysers (Kozlova and Manning, 2009), albeit possibly at reduced frequency. [In this paper we quantify the compatibility, repeatability, The accuracy, precision, and drift rates are quantified and presented here](#) in the context of [the WMO/GAW guidelines](#) (Crotwell et al., 2019). In order to further examine the performance of the G2207-*i* 105 in real-world applications, we also calculated ffCO₂ from concurrent O₂ and CO₂ measurements [made](#), using the novel methodology presented by Pickers et al. (2022). We compare ffCO₂ calculated with O₂ measurements from the G2207-*i* installed at WAO with ffCO₂ calculated from the established O₂ system employing a Sable Systems International Inc. “Oxzilla 110 II” fuel cell analyser.

2 Methods

2.1 Picarro G2207-*i* O₂ analyser

110 The Picarro G2207-*i* O₂ analyser measures the mole fractions of the two most abundant atmospheric O₂ isotopologues, ¹⁶O¹⁶O and ¹⁶O¹⁸O, through absorption spectra at 7882.18670 cm⁻¹ and 7882.050155 cm⁻¹, respectively (Berhanu et al., 2019). The design principles of this analyser have been described in detail by Berhanu et al. (2019). In our study we evaluate only what is called the “O₂ concentration” mode, measuring only the ¹⁶O¹⁶O isotopologue. In the other mode, called the “δ¹⁸O plus O₂ concentration” mode, O₂ mole fraction values are considerably less precise, as the analyser is not optimised for ¹⁶O¹⁶O 115 measurements (primarily via a different set point for the pressure in the cavity). The analyser reports both “wet” and “dry” O₂ mole fraction values. The “wet” values (O_{2,NC}) do not have any correction applied to them, whereas the “dry” values (O_{2,WC}) are corrected for the dilution effect of water vapour on the O₂ mole fraction, as well as spectroscopic interference, using the analyser’s parallel water vapour mole fraction measurements. [The G2207-*i* datasheet states a measurement precision of 5 ppm + 0.1 % of the reading \(1- \$\sigma\$, 5 sec\) for the water vapour mole fraction.](#)

120 2.2 CRAM laboratory measurement of cylinder gases

The performance of the G2207-*i* was evaluated in the UEA CRAM Laboratory by measuring a suite of 12 gas cylinders all 125 containing dry natural air with varying O₂ mole fractions. The cylinders were stored horizontally in a thermally insulated “Blue Box” enclosure in order to prevent gravitational and thermal fractionation of O₂ relative to N₂ (Keeling et al., 2007). The O₂ composition of each of these cylinders was precisely defined on the Scripps Institution of Oceanography (SIO) O₂ scale (Keeling et al., 2007) using a VUV O₂ analyser, also in the CRAM Laboratory. The CO₂ mole fraction was defined on the “WMO CO₂ X2007” scale (Zhao and Tans, 2006) using a Siemens Corp. Ultramat model 6F non-dispersive infrared (NDIR) CO₂ analyser. Five of these cylinders were working secondary standards (WSSes) which were used to calibrate the G2207-*i*, one was a reference tank (RT; explained below in section 2.3.2), and the other six were treated as cylinders with unknown mole fractions ([Table 1](#)[Table 4](#)). The six “unknown” cylinders were used to evaluate the performance of the analyser with a

130 CO₂ mole fraction range of 375 to 443 ppm and an O₂/N₂ ratio range of -915 to 435 per meg, a much larger range than would typically be observed in ambient air.

The cylinders were run consecutively, starting with the six “unknowns” and ending with the [5-five](#) WSSes, with the RT run at the beginning and end, this was repeated twice. Each of the gas cylinders was flushed for 20 minutes prior to running on the G2207-*i* to allow for removal of stagnant air and equilibration of the pressure regulators; air from each cylinder was then 135 passed through the analyser for 20 minutes, with the first 8 minutes of data discarded to allow flushing of the previous cylinder’s air from the cavity, [and to maintain consistency with the purging period during the flushing time employed in subsequent WAO tests \(section 2.3.2\)](#). The remaining 12 minutes for each cylinder was then averaged to give the “raw” O_{2,NC} value for each cylinder as measured on the G2207-*i*.

140 **Table 1. Declared O₂/N₂ ratios and CO₂ mole fractions with $\pm 1\sigma$ standard deviations of the five WSSes, RT, and six “unknown” cylinder gases used in the CRAM Laboratory tests of the G2207-*i***

Cylinder number	Cylinder ID	Declared O ₂ (per meg) ^a	Declared CO ₂ (ppm) ^b
WSS1	D089507	-565.5 \pm 1.3	428.741 \pm 0.018
WSS2	D801299	-486.1 \pm 3.0	381.230 \pm 0.016
WSS3	D073409	-658.4 \pm 2.2	398.875 \pm 0.018
WSS4	D073419	-926.4 \pm 5.9	440.355 \pm 0.072
WSS5	D073418	-782.7 \pm 5.6	413.662 \pm 0.057
RT	CC78691	-414.3 \pm 0.8	384.915 \pm 0.005
1	D273555	-914.8 \pm 0.7	443.384 \pm 0.013
2	D399093	-880.5 \pm 0.9	415.246 \pm 0.003
3	ND29112	-582.0 \pm 1.0	399.976 \pm 0.004
4	ND29110	-375.0 \pm 1.3	381.544 \pm 0.004
5	D273559 ^c	411.7 \pm 2.1	375.122 \pm 0.007
6	D801298 ^c	434.6 \pm 0.3	412.934 \pm 0.002

^aValues declared with a VUV O₂ analyser in the CRAM Laboratory traceable to the SIO O₂ scale

^bValues declared with a Siemens Ultramat 6F NDIR CO₂ analyser in the CRAM Laboratory traceable to the WMO CO₂ X2007 scale

145 ^cThe O₂ values of these cylinders is far outside the range observed in ambient air, thus are less relevant to the applications of atmospheric observations but have been included in this analysis for completeness of examining the analysers performance.

The G2207-*i* has a linear response to O₂ mole fraction (Eq. (3))

$$y = Bx + C \quad (3)$$

where, B and C are the coefficients derived from the slope and intercept of the linear regression calculated from the 150 measurement of the WSSes. Therefore, a minimum of two WSS cylinders are required to determine the B and C coefficients,

but by using five we are able to calculate the coefficient of determination (R^2), as well as providing more robustness in the fit. The calibration equation was used to convert the “raw” $O_{2,NC}$ values taken from the G2207-*i* (“x” in Eq.(3)) into what we call “ppm equivalent” (ppmEquiv) O_2 units (“y” in Eq. (3)), as described in Kozlova and Manning (2009). A linear interpolation between the RT at the beginning and end of each run was used as a baseline for the run and subtracted from all other cylinder measurements to correct for short-term [instrumental-analyser](#) variations. The calibration curve (Eq. (3)) for the G2207-*i* was also determined relative to the interpolated RT values (WSS - RT), thus all the unknown cylinder measurements could be converted into ppmEquiv. The ppmEquiv O_2 units were then converted to per meg units, providing a $\delta(O_2/N_2)$ value for each “unknown cylinder, using Eq. (4).

$$\delta \left(\frac{O_2}{N_2} \right) = \frac{\delta O_2 + (CO_2 - 363.29) \times S_{O2}}{S_{O2} \times (1 - S_{O2})} \quad (4)$$

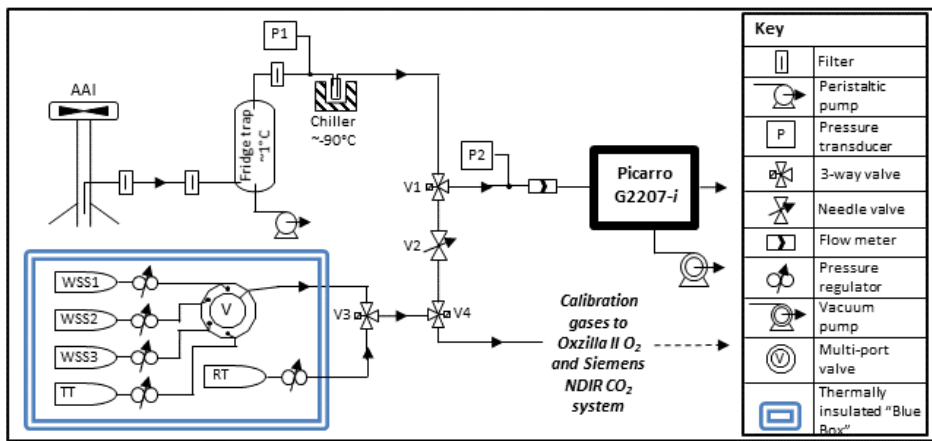
160 where, δO_2 is the calibrated G2207-*i* $O_{2,NC}$ values in ppmEquiv units, CO_2 is the declared cylinder CO_2 mole fraction from the Siemens analyser in ppm, S_{O2} is 0.2094, which is the standard mole fraction of O_2 molecules in dry air (Tohjima et al., 2005), and 363.29 is an arbitrary CO_2 reference value in ppm, inherent to the SIO O_2 scale (Stephens et al., 2007).

2.3 Weybourne Atmospheric Observatory field tests

165 Weybourne Atmospheric Observatory (WAO) is located on the north Norfolk coast, UK (52°57'02"N, 1°07'19"E), approximately 35 km north-northwest of Norwich, 170 km northeast of London and 200 km east of Birmingham. It is part of the European Union’s Integrated Carbon Observation System (ICOS) and the World Meteorological Organization’s (WMO) Global Atmosphere Watch (GAW) programme. High-precision, high-accuracy, continuous measurements of a wide array of atmospheric gas species (including greenhouse gases, isotopes, reactive gases) are carried out at a fine temporal scale, funded in part through the UK’s National Centre for Atmospheric Science (NCAS) long-term measurement programme.

170 Atmospheric O_2 and CO_2 have been measured continuously at WAO since 2008 (Wilson, 2013). O_2 is measured with a “Oxzilla II” O_2 analyser (Sable Systems International Inc.) (hereafter referred to as the “Oxzilla”), and CO_2 is measured with an Ultramat 6E NDIR analyser (Siemens Corp.). These analysers are in series, with the air sample first passing through the Ultramat 6E and then the Oxzilla, with rigorous gas handling and calibration protocols followed (as in Stephens et al., 2007).

175 The G2207-*i* was installed at WAO from 23 October 2019 – 02 November 2019, sampling from a solar shield aspirated air inlet (AAI) at a height of 10 m above ground level (AGL) (20 m above sea level (ASL)). The AAI protects the inlet from solar radiation and generates a continuous air flow over the inlet, thus preventing the differential fractionation of O_2 molecules relative to N_2 molecules due to ambient temperature variations (Blaine et al., 2006) and relatively slow inlet flow rates (Manning, 2001). A [full_plumbing](#)-diagram of the gas-handling set-up [for the G2207-*i*](#) at WAO is displayed in Fig. 1.



|180 Figure 1: Gas handling [plumbing](#) diagram of the Picarro G2207-i installed at WAO. (AAI, aspirated air inlet; WSS, working secondary standard; RT, reference tank; TT, target tank). Calibration gases were shared with the established O₂ and CO₂ system (using V4), but [the established system has its own AAI, pump, drying system, and pressure and flow control \(not depicted here\)](#).

2.3.1 Drying

Water vapour mole fractions in the troposphere vary from a few ppm to a few percent over small temporal and spatial scales.¹⁸⁰

185 This water vapour has a diluting effect on atmospheric gas measurement. A 1 ppm increase of water vapour will dilute the measured atmospheric O₂ by approximately 1.3 per meg (Stephens et al., 2007); [so](#) the existing method for high-precision atmospheric O₂ measurements is therefore to dry the sample air to less than 1 ppm [water vapour content](#) before measurement [in order to prevent the dilution effect of water vapour](#). All calibration and RT gases are also dried to less than 1 ppm water vapour. Furthermore, measurements using spectroscopy techniques are also sensitive to water vapour variability due to changes 190 in the degree of pressure broadening of the spectroscopic lines used to measure the O₂ and δ¹⁸O₂. Water vapour correction has previously been successfully implemented for measurements of CO₂ and methane (CH₄) with CRDS analysers (Chen et al., 2010); however, in order to achieve accuracies within the WMO goal of 1% H₂O custom coefficients must be obtained for each analyser (Rella et al., 2013).

195 As discussed in section 2.1, O₂ measurements are reported by the G2207-i as “wet” (O_{2,NC}) and, after the implementation of water correction, “dry” (O_{2,wc}). In order to evaluate the effectiveness of the built-in water correction procedure for compensating for water vapour dilution, ambient air was sampled with three different drying regimes: no drying, partial drying, and full drying. Under the full drying conditions (which is the current standard practice), the sample air passed through a fridge trap (~1°C) and a cryogenic chiller trap (~-90°C), removing water vapour to < 1 ppm. Under partial drying the chiller was bypassed, so the sample air only passed through the fridge trap which dries the air to approximately 5000 ppm of water vapour.

200 With no drying, both the chiller and fridge were bypassed. Air was simultaneously sampled through a separate AAI (10 m AGL) into the pre-existing O₂ and CO₂ system with full drying during each of these stages. The time difference between air travelling from the AAIs to each of the two analysers was accounted for.

To evaluate the built-in water correction procedure of the G2207-*i* the O_{2,WC} values were compared with measurements from the Oxzilla (which was continuously sampling fully dried air) for the no drying and partial drying periods, and the O_{2,NC} and 205 O_{2,WC} G2207-*i* values were compared to the Oxzilla when sampling fully dried air.

2.3.2 Calibration procedure

A tailor-made calibration protocol was developed for the G2207-*i* following ICOS atmospheric station specifications (Icos-Ri, 2020). The calibration cylinders were stored horizontally in a thermally insulated “Blue Box” enclosure in order to prevent gravitational and thermal fractionation of O₂ and N₂. The calibration gases consisted of three WSSes with precisely defined 210 O₂ and CO₂ values which span the unpolluted atmospheric range (traceable to the SIO O₂ and WMO CO₂ X2007 scales) and a reference tank (RT) with O₂ and CO₂ values close to ambient air conditions at the site. The repeatability and compatibility of the analyser were evaluated using a target tank (TT) ([sometimes known as a “surveillance tank”](#)) with precisely defined O₂ and CO₂ values. With full drying of the sample air each of the WSSes, the RT, and the TT were run for 20 minutes, the first 8 minutes was discarded due to the sweep-out time of the G2207-*i*, [equilibration after valve switching, and surface effects](#), and 215 the final 12 minutes averaged to determine the cylinder value for the given run. [A flushing period of 8 minutes and averaging time of 12 minutes were chosen to match that of the established system](#). Under partial and no drying the run-time of the cylinders was increased in order to fully flush the G2207-*i* of water vapour; each cylinder was therefore run for 32 minutes, with the first 20 minutes being discarded and the final 12 minutes averaged.

A full 3-gas WSS calibration of the G2207-*i* was run every 23 hours, this frequency is intentionally not a multiple of 24 hours 220 in order to prevent aliasing the data by calibrating under environmental conditions that may occur at the same time each day. This calibration corrects for drift in the span or non-linearity of the analyser. As in the CRAM laboratory tests (see section 2.2), the WSSes were used to define a calibration equation to convert the raw analyser O₂ values into ppmEquiv O₂ units. Eq. (3) and the concurrent CO₂ measurement from the Ultramat 6E NDIR were then used to convert this into per meg units.

The RT is used for data correction caused by short-term [instrument analyser](#) drift and was run every 5 hours. A linear 225 interpolation between each of the RT run averages was treated as a baseline and subtracted from all subsequent air and cylinder measurements. The calibration curve for the G2207-*i* was also determined relative to the RT values (WSS- RT) , thus the air measurement differences can be easily converted into per meg units.

Finally, the TT was run every 7 hours, this cylinder is used to quantify the repeatability and compatibility of the analyser. “Repeatability” is defined as the closeness of agreement between results of successive measurements of the same measure 230 carried out under the same measurement conditions and is considered as a proxy for the precision of a measurement system. “Compatibility” is defined as the averaged O₂ value of all TT runs over time, compared to the values declared by the VUV, and provides a measure of the compatibility to the SIO scale over time (Kozlova and Manning, 2009). The TT air does not

pass through the AAI or drying lines (Fig. 1) so it is therefore mainly representative of the analyser's repeatability and compatibility only.

235 2.5 Quantifying fossil fuel CO₂ using atmospheric potential oxygen

In order to further assess the G2207-*i*'s performance in real-world applications the O_{2,NC} observations from the full drying regime period at WAO were used to isolate the fossil fuel component of the concurrent CO₂ observations and then compared to the ffCO₂ values calculated from atmospheric potential oxygen (APO) derived from the Oxzilla O₂ observations following the methodology outlined in Pickers et al. (2022).

240 The tracer APO, derived by Stephens et al. (1998), was first calculated using Eq. (45) (using both G2207-*i* O_{2,NC} and Oxzilla O₂ values); these APO values were then used to calculate ffCO₂ using Eq. (56).

$$APO = [O_2] + \left(\left(\frac{-1.1}{0.2094} \right) \times (350 - [CO_2]) \right) \quad (45)$$

245 where O₂ and CO₂ are in per meg and ppm units, respectively; -1.1 is the global average O₂:CO₂ terrestrial biosphere-atmosphere exchange rate (Severinghaus, 1995), 0.2094 is the standard mole fraction of O₂ molecules-in dry air (Tohjima et al., 2005), and 350 is an arbitrary reference value for CO₂ in ppm. Multiplying CO₂ by -1.1 and dividing by 0.2094 converts the CO₂ data from ppm to per meg units.

$$ffCO_2 = \frac{APO - APO_{bg}}{R_{APO:CO_2}} \quad (56)$$

250 Where APO is derived from Eq. (45) in per meg units, APO_{bg} is the APO background, or baseline, value determined using a statistical baseline fitting procedure, and R_{APO:CO₂} is the APO:CO₂ combustion ratio for fossil fuel emissions. The APO_{bg} values were determined using the rfbaseline function from the IDPmisc package in R, which implements robust fitting of local regression models, with a smoothing window of one week (Ruckstuhl et al., 2012). The APO:CO₂ emission ratio (R_{APO:CO₂}) used is -0.3 mol mol⁻¹, an approximate mean value for WAO as determined from the COFFEE inventory (a typical value for fossil fuel emissions, given that the APO:CO₂ ratio = O₂:CO₂ + 1.1) (Pickers, 2016; Steinbach et al., 2011). The uncertainty on the ffCO₂ mole fractions was calculated using Eq. (56) with the upper and lower uncertainty limit for each variable (where the measurement uncertainty for APO was calculated by summing in quadrature the CO₂ and O₂ measurement uncertainty for each analyser), then taking the SD of the resultant ffCO₂ value for of each combination for each hourly time stamp.

3. Results and discussion

3.1 Precision and drift

260 To assess the short-term precision and optimal averaging time of the G2207-*i* the Allan deviation technique (Werle et al., 1993) was used whilst sampling a compressed-air cylinder in the laboratory (50 L, 200 bar). The cylinder was run for 24 hours with a sample flow rate of 94 mL⁻¹ min⁻¹ and cavity pressure and temperature of 255 torr and 45°C, respectively. The results of this

Allan deviation analysis are in agreement with those obtained by Berhanu et al. (2019), where a precision of 1 ppm (~4.8 per meg) was achieved after an averaging time of 300 seconds. Precision then continues to improve until around a 30 minute averaging time where a precision of ~0.5 ppm (~2.4 per meg) is reached, and remains around that value for averaging times up to around 1 hour (Figure 2), and continues to improve until around 3000 seconds where a precision of ~0.3 ppm (~1.44 per meg) is reached (Figure 2). It should be noted, that unlike the hourly average and standard deviation obtained from measurement of cylinder air, the hourly averages of atmospheric data also contain natural variability in addition to analyser-related noise and drift.

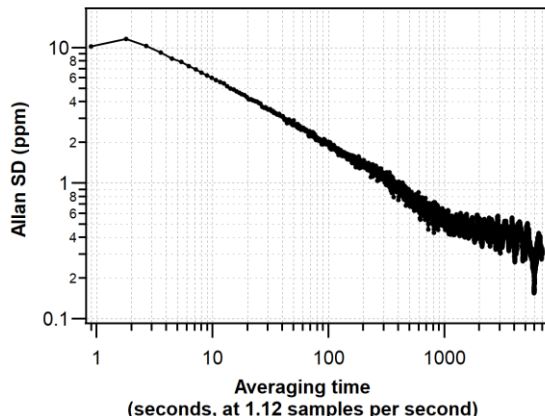
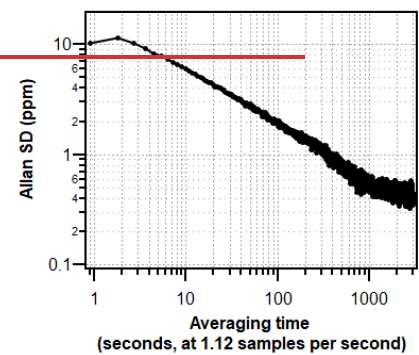


Figure 2. Allan deviation plot displaying the precision of the G2207-i O₂ mole fraction measured from an ambient compressed-air cylinder.

To evaluate the analyser drift (i.e., the changing sensitivity of the analysers response with time), $O_{2,NC}$ values from the G2207-*i* were averaged to 1 hour (Fig. 3b; reported in ppm where 1 ppm corresponds to a change of 4.8 per meg in the O_2/N_2 ratio).

275 The G2207-*i* datasheet states a maximum drift at STP (over 24 hours, peak-to-peak, 1-hour internal average at 21 % O_2) of <6 ppm. We found that over 24 hours, the maximum peak-to-peak drift of the hourly averages is ~1.2 ppm (approximately 5.76 per meg); this is better than stated by Picarro Inc. but does not meet the WMO compatibility goal of ± 2 per meg, as the internal drift of the analyser is greater than this goal. The standard deviation of each of these hourly averages is ~14.5 ppm (~69.6 per meg) (Fig. 3a), this is caused by the large amount of analyser noise in the raw 1 second data points, spanning ~100 ppm (~480 per meg) (Fig. 3c). The overall drift over the 24 hours of raw data however is very small, shown by a linear regression slope of $-4.26 \times 10^{-6} \text{ ppm s}^{-1}$ (Fig. 3c).

Formatted: Superscript

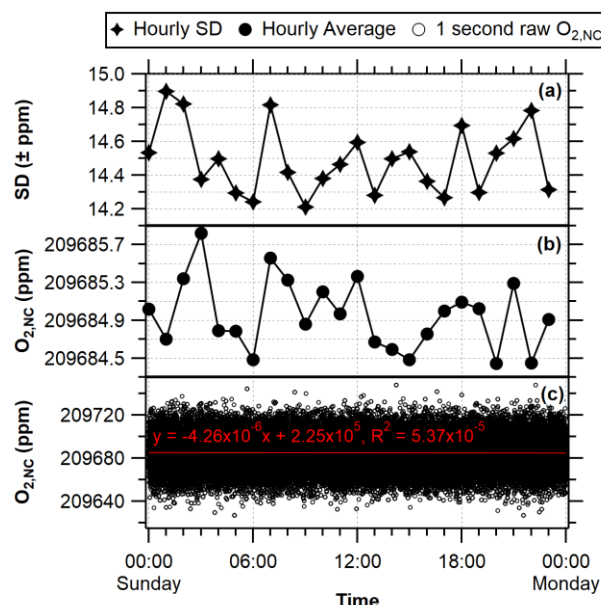


Figure 3. $O_{2,NC}$ mole fractions from the G2207-*i* sampling dry compressed cylinder air over 24 hours, reported in ppm, where 1 ppm corresponds to a change of 4.8 per meg in the O_2/N_2 ratio. (a) Standard deviation of the hourly averaged values. (b) Hourly averaged $O_{2,NC}$. (c) Raw 1 second $O_{2,NC}$ values, the red line depicts the linear regression line, with the equation and R^2 value written above.

3.2 CRAM laboratory measurement of cylinder gases

The G2207-*i* analyser performance was evaluated by measuring six gas cylinders with precisely defined O_2 and CO_2 values as measured on a VUV O_2 analyser and Siemens Ultramat 6F NDIR CO_2 analyser (Table 1 Table 4). The difference between the

Formatted: Font: Italic

Formatted: Subscript

Formatted: Subscript

Formatted: Subscript

Formatted: Subscript

290 O_2 values (per meg) as measured by the G2207-*i* and the declared values from the VUV are shown in Table 2, for both runs
with and without the RT interpolation applied.

Formatted: Subscript

Formatted: Font: Italic

For both runs without the application of the RT interpolation the difference between the VUV declared value and that measured
by the G2207-*i* is very large, and far outside of an acceptable range (Table 2), with an average difference from the declared
values for all cylinders of 22.0 ± 10.3 per meg. For all cylinders, except for cylinder 5 and 6, a large improvement in the
difference is seen after the application of the RT correction. Due to the large differences between the declared and measured
values without the RT correction applied, only the results with the RT correction will be discussed hereafter.

Formatted: Font: Italic

295 **Table 2. The difference between the O_2 value of each cylinder as measured on the G2207-*i* and the VUV analyser (G2207-*i* - VUV),
for two runs on the G2207-*i* with and without RT correction applied.**

Cylinder no.	O ₂ (per meg)	Without RT correction			With RT correction		
		Run 1 difference from Declared	Run 2 difference from Declared	Mean of absolute differences of both runs	Run 1 difference from Declared	Run 2 difference from declared (per meg) ^a	Mean of absolute differences of both runs (per meg) ^b
		(per meg) ^a	(per meg) ^a	(per meg) ^b	(per meg) ^a	(per meg) ^a	(per meg) ^b
1	-914.8 \pm 0.7	9.9 \pm 8.4	21.4 \pm 8.2	15.7 \pm 8.1	0.4 \pm 8.5	2.4 \pm 8.1	1.4 \pm 1.4
2	-880.5 \pm 0.9	13.7 \pm 8.7	26.5 \pm 8.3	20.1 \pm 9.1	6.1 \pm 8.4	7.6 \pm 8.2	6.9 \pm 1.1
3	-582.0 \pm 1.0	8.1 \pm 8.5	22.4 \pm 11.3	15.3 \pm 10.1	0.7 \pm 8.0	3.1 \pm 11.2	1.9 \pm 1.7
4	-375.0 \pm 1.3	12.4 \pm 11.6	18.4 \pm 9.5	15.4 \pm 4.2	5.8 \pm 11.3	-1.1 \pm 9.5	3.5 \pm 3.3
5	411.7 \pm 2.1	44.0 \pm 12.6	-3.6 \pm 11.5	23.8 \pm 28.6	19.0 \pm 12.4	-40.1 \pm 10.2	29.6 \pm 14.9
6	434.6 \pm 0.3	44.6 \pm 5.4	-39.1 \pm 10.2	41.9 \pm 3.9	22.2 \pm 5.1	-49.8 \pm 11.5	36.0 \pm 19.5

^a $\pm 1\sigma$ standard deviation of the 12-minute G2207-*i* average.

^b $\pm 1\sigma$ standard deviation of the average of the run 1 and run 2 G2207-*i* - VUV absolute differences.

300 Cylinders 5 and 6 contain an O_2 values far higher than that found in ambient air (411.7 and 432.6 and per meg, respectively) and outside of the range spanned by the WSSes used for calibration. For these two cylinders, the difference between the declared value and that measured by the G2207-*i* is far larger than the other cylinders and also more variable between the two runs with a standard deviation of the absolute values between the two runs of ± 14.9 and 36.0 ± 19.5 per meg, respectively
305 (Table 2). Berhanu et al. (2019) found that the accuracy of the G2207-*i* was reduced when the CO_2 mixing ratio was much higher than that of ambient air but did not observe the same reduction in accuracy with high O_2 mixing ratios. Ignoring the two cylinders with positive O_2 , the average absolute difference between the remaining 4 unknown cylinders and the declared values over the two runs is 3.4 ± 2.5 per meg, this is slightly greater than the WMO compatibility goal of ± 2 per meg but does fall within the extended goal of ± 10 per meg and is similar to what can be achieved with an Oxzilla II (Pickers et al., 2017).

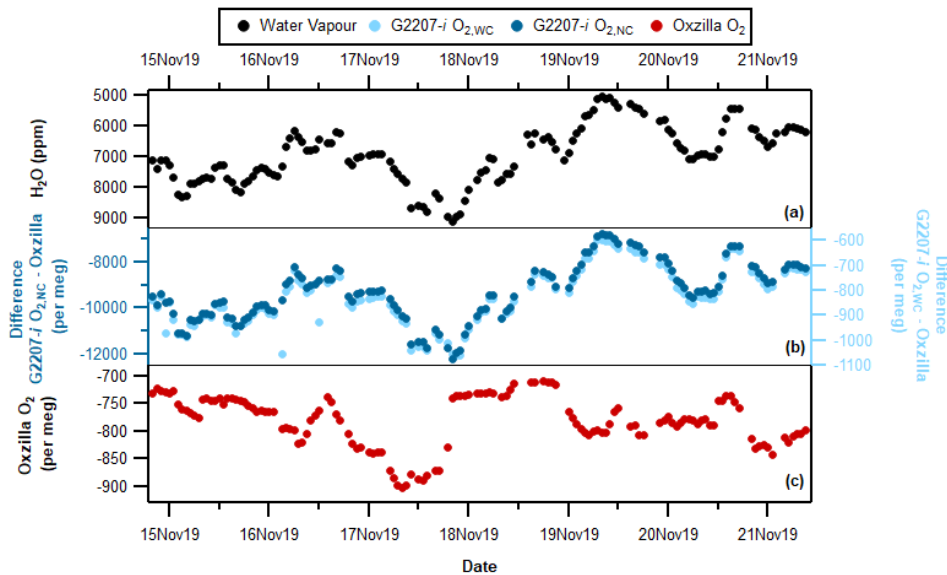
310 There is also no correlation between the accuracy and the declared O₂ value excluding the two cylinders with positive O₂ (R² = 0.07 for run 1, R² = 0.53 for run 2).

Although the accuracy of the O₂ values measured by the G2207-*i* for these cylinders is variable, particularly for the cylinders with high O₂, the standard deviation of the 2-minute data points used to calculate the final cylinder O₂ value as defined by the G2207-*i* within each run is more consistent. However, the repeatability, used as a proxy for precision, and defined here as the 315 $\pm 1\sigma$ standard deviation of the average of the two measurements of each cylinder are variable. For the two cylinders with high O₂ (cylinders 5 and 6) the repeatability is more than 5 times greater than the WMO extended repeatability goal of ± 5 per meg. For the remaining four cylinder the repeatability is far lower, with cylinder 1 and cylinder 3 both falling within the extended repeatability goal.

3.3 Weybourne Atmospheric Observatory field tests

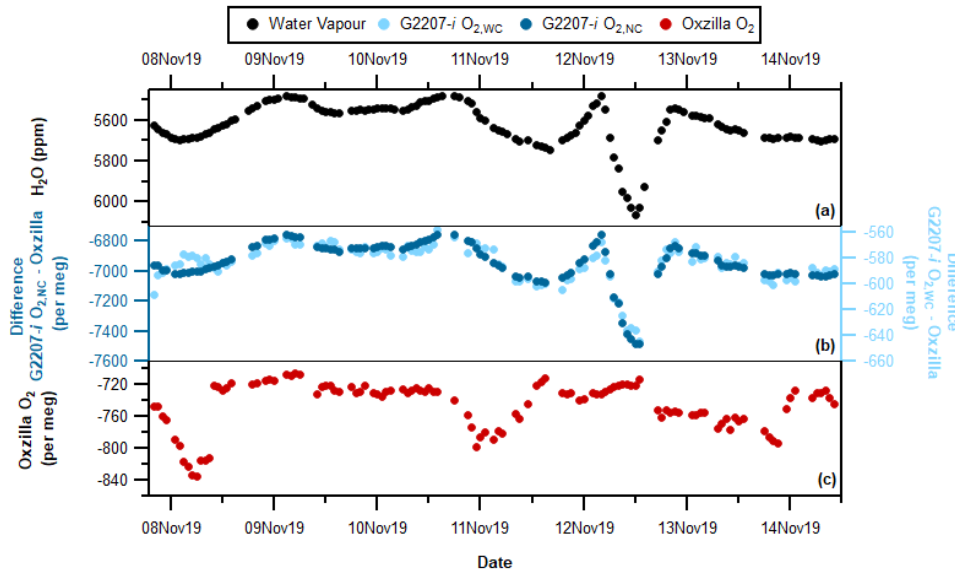
320 3.3.1 Partial and no drying of ambient air measurements

The results from no drying and partial drying of the sample air into the G2207-*i* at WAO are displayed in Fig. 4 and Fig. 5, respectively. The O₂ mole fractions reported in ppm units by the G2207-*i* were converted to per meg units using the calibration equations produced through the measurement of the three WSS cylinders every 23 hours, and the concurrent CO₂ observations.



325 **Figure 4.** (a) Hourly averaged water vapour, (b) G2207-*i* – Oxxilla difference for $O_{2,NC}$ (dark blue) and $O_{2,WC}$ (light blue), and (c) Oxxilla O_2 with no drying of the sample air through the G2207-*i*. N.B., the reversed water vapour axis and different axis scales for $O_{2,NC}$ and $O_{2,WC}$.

During the period where there was no drying of the G2207-*i* air sample there is a significant difference between the O_2 values reported by the Oxxilla (dried air) and the G2207-*i* $O_{2,NC}$ values (Fig. 4b), this is to be expected due to the diluting effect of 330 water vapour; however, there is also a significant difference between the Oxxilla O_2 and the G2207-*i* $O_{2,WC}$ values. Over the entire no drying period the average difference between the Oxxilla observations and the G2207-*i* $O_{2,NC}$ is -9654.41 ± 272.84 per meg. The average difference between the Oxxilla and the G2207-*i* $O_{2,WC}$ values is -849.78 ± 31.12 per meg. Although the difference is substantially smaller with the application of the G2207-*i* built-in water correction procedure, it is still unusably large, with no similarity in the Oxxilla and G2207-*i* signals and both the $O_{2,NC}$ and $O_{2,WC}$ G2207-*i* values correlating with the 335 H_2O variability (Fig. 6e-6a and 6b). This demonstrates that the algorithm currently applied for water correction is unsuitable for precise O_2 measurement.



340 **Figure 5.** (a) Hourly averaged Water vapour (top), (b) G2207-*i* – Oxxilla difference for $O_{2,NC}$ (dark blue) and $O_{2,WC}$ (light blue), and (c) Oxxilla O_2 (bottom) with partial drying of the sample air through the G2207-*i* (Oxxilla sample air is fully dried). N.B., the reversed water vapour axis, and different axis scales for $O_{2,NC}$ and $O_{2,WC}$. The spike in water vapour on 12 November 2019 is due to a temporary increase in the temperature of the fridge.

As seen during no drying of the sample air, there is also a significant difference between the reported O_2 values of the Oxxilla and G2207-*i* under the partial drying regime, for both $O_{2,NC}$ and $O_{2,WC}$ (Fig. 5b). With partial drying the time-series of the

difference between the O_2 values of the two analysers is a lot smoother than with no drying, this is due to the fridge trap
345 removing some of the natural variability in the water vapour mole fraction. Over the entire partial drying period the average
difference between the Oxzilla observations and the G2207-*i* $O_{2,NC}$ is -7144.06 ± 258.60 per meg. The average difference
346 between the Oxzilla and the G2207-*i* $O_{2,WC}$ values is -612.71 ± 31.77 per meg. There is a large improvement with the
application of the water correction procedure; however, as with the no drying results, the difference in O_2 values between the
347 Oxzilla and G2207-*i* $O_{2,WC}$ are too large to be usable for any application, with the $O_{2,NC}$ and $O_{2,WC}$ values correlating with the
348 H_2O variability (Fig. 6a-6c and 6d), and therefore will not be investigated further.

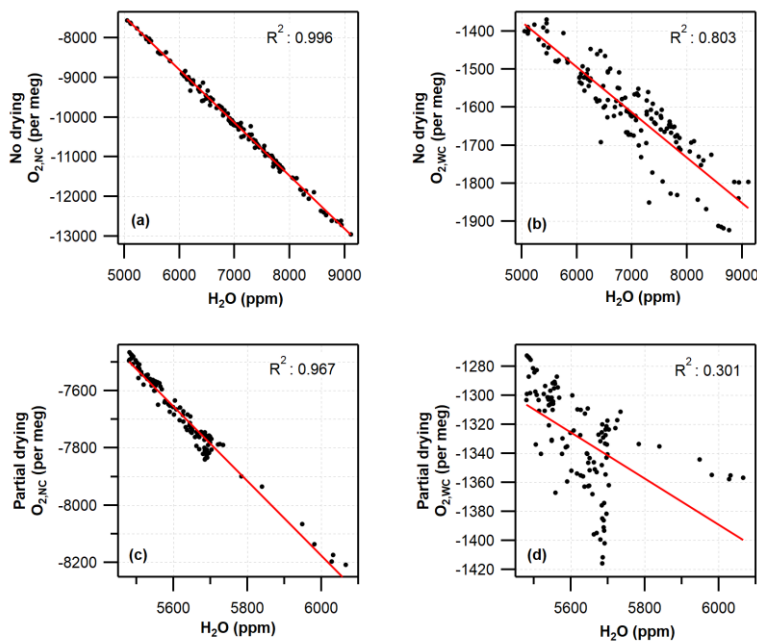


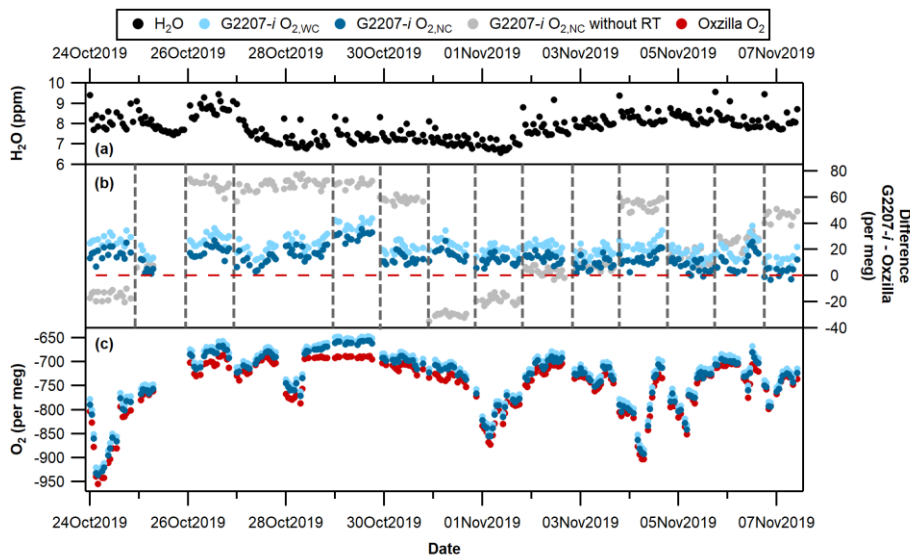
Figure 6. Correlation between water vapour mole fraction and hourly averaged G2207-*i* O_2 for (a) no drying $O_{2,NC}$, (b) no drying $O_{2,WC}$, (c) partial drying $O_{2,NC}$, and (d) partial drying $O_{2,WC}$. Red lines show linear regression.

Under both “partial drying” and “no drying” regimes, the difference between the Oxzilla and G2207-*i* values is strongly
355 correlated with the water vapour mole fraction but decreases with the application of the built-in water correction procedure
(Fig. 6). The R^2 value decreases from 0.996 to 0.803 for no drying and from 0.967 to 0.301 for partial drying once the water
correction has been applied. Given the correlation between the water vapour mole fraction and the $O_{2,WC}$ reported by the
356 G2207-*i* these values are not usable without significant improvements to the water correction procedure by Picarro Inc..

Due to the large differences observed between the Oxzilla and G2207-*i* reported O₂ values under no drying and partial drying,
360 no further investigation was undertaken, thus only the fully dried sample air is considered hereafter.

3.3.2 Full drying of ambient air measurements

The results from fully drying the sample air between 24 October 2019 and 07 November 2019 are displayed in Fig. 7. The O₂ mole fractions reported in ppm units by the G2207-*i* were converted to per meg units using the calibration equations produced through the measurement of the three WSS cylinders every 23 hours, and the concurrent CO₂ observations.



365
370 **Figure 7.** Time-series with full drying of the air sample. (a) Hourly averaged water vapour, spikes are due to equilibration after valve switching from cylinder air to sample air. (b) G2207-*i* – Oxzilla difference for O₂,WC (light blue), O₂,NC (dark blue), and O₂,NC without the RT interpolation applied (grey); vertical dashed lines indicated a full 3-gas WSS calibration on the G2207-*i*, and the red horizontal line indicates zero difference from the Oxzilla. (c) Hourly averaged Oxzilla O₂ (red), O₂,WC (light blue) and O₂,NC (dark blue). Note, there was no WSS calibration on 27 October 2019 due to a macro error which prevented valve switching to calibration gases, therefore the calibration from 26 October 2019 was applied for 46 hours.

There is a greater difference between the Oxzilla and G2207-*i* O₂,WC values than the O₂,NC values, with an average difference over the entire full drying period of 22.60 ± 7.41 per meg compared to 13.59 ± 7.46 per meg, respectively. This may be due to overcorrection of the O₂,NC values as the water vapour mole fraction is below the G2207-*i*'s lower detection limit [and precision](#)
375 i.e. the G2207-*i* is reporting H₂O mole fractions of approximately 7 ppm (Fig. 7a) (with frequent spikes due to equilibration when the air sample is fully dried by passing through the

chiller and fridge trap, the water vapour is reduced to below 1 ppm. This overestimated water correction whilst sampling fully dried air was also found by Berhanu et al. (2019). We therefore only refer to the $O_{2,NC}$ values, which we believe to be more accurate, in the analysis from now onwards.

380 The large jumps in the G2207-*i* $O_{2,NC}$ values following WSS calibrations (see Fig. 7b, grey points) are caused by a drift in the instruments-analyser's baseline, [which only becomes applied to the data after each calibration](#). These jumps were reduced through the application of the 5-hour RT interpolation procedure ([see Figure 7b, blue points](#)) [which constrained the baseline drift](#) (refer to Section 2.3.2). After the application of the RT interpolation the jumps between WSS calibrations were vastly reduced (see Fig. 7), thus the $ffCO_2$ results in section 3.5 have this applied.

385

3.3.3 Repeatability and compatibility

The repeatability and compatibility of the analyser were evaluated through the running of a TT every 7 hours during the full drying period using $O_{2,NC}$ values, the results of which are presented in Fig. 8 and Table 3. For O_2 the WMO repeatability goal is ± 1 per meg (with an extended goal of ± 5 per meg) and the compatibility goal is ± 2 per meg (with an extended goal of \pm

390 10 per meg) (indicated by the [grey](#)-dashed lines in Fig. 8) (Crotwell et al., 2019).

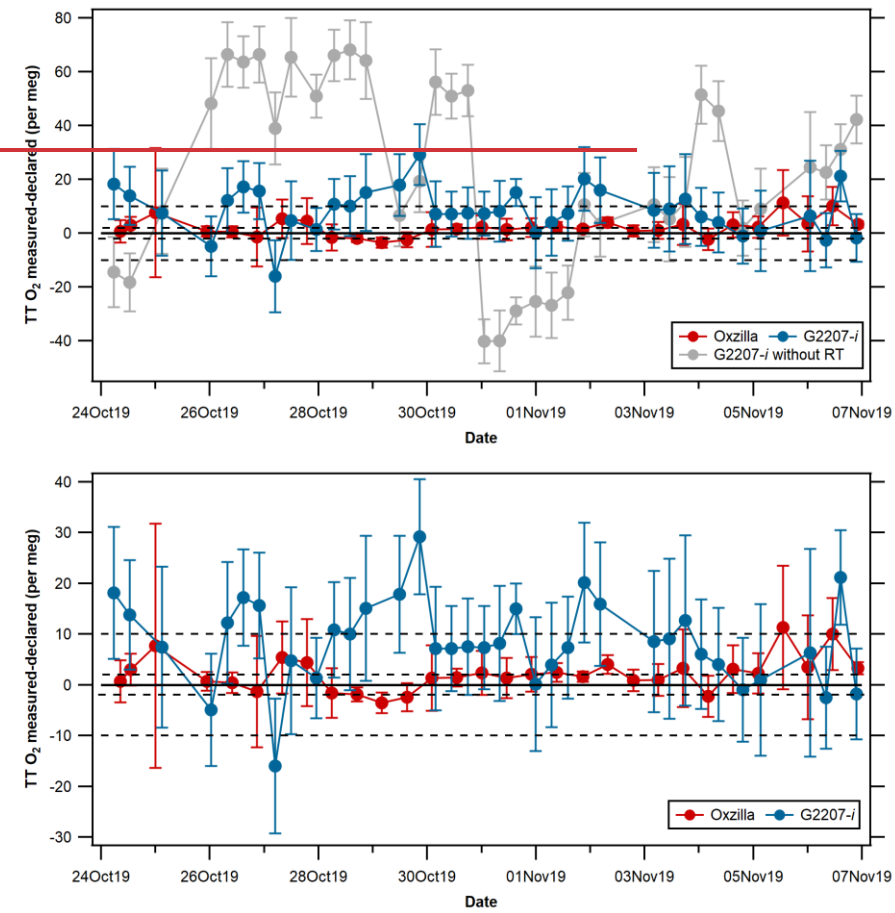


Figure 8. TT differences from declared values (measured - declared) ($\pm 1\sigma$ standard deviation) for the Oxzilla (red) and G2207-i O_2 NC (blue), and G2207-i O_2 NC without RT (grey). The solid line indicates zero difference from the declared O_2 value of the TT, and the dashed lines indicate the WMO compatibility goal of ± 2 per meg and the extended goal of ± 10 per meg.

395

Table 3. Repeatability and compatibility goals, and achievements for each analyser

	Repeatability (per meg) ^a	Compatibility (per meg) ^b
WMO compatibility goal	$\pm 1 (\pm 5)^c$	$\pm 2 (\pm 10)^c$

Oxzilla	$\pm 2.21 \pm 1.96$	$\pm 3.03 \pm 2.59$
G2207- <i>i</i> O _{2,NC} without RT interpolation	$\pm 11.86 \pm 13.83$	$\pm 22.88 \pm 34.11$
G2207- <i>i</i> O _{2,NC}	$\pm 5.69 \pm 5.61$	$\pm 9.97 \pm 6.71$

^a Values are calculated using the method in Kozlova and Manning (2009) and Pickers et al. (2017). Mean $\pm 1\sigma$ standard deviations of the average of two consecutive measurements of the TT, determined from 30 TT measurements for the Oxzilla and 37 TT measurements for the G2207-*i*, where one run is the average of 12 minutes of data. Uncertainties are given on these

400 mean standard deviations, illustrating that the analytical repeatability is variable over time.

^b Mean differences between the measured TT O₂/N₂ ratio, and the declared values determined on the VUV analyser against primary calibration standards on the SIO O₂ scale.

^c WMO repeatability and compatibility goals, where the repeatability of a measurement should be at most half of the value of the compatibility goal. For O₂, the WMO the goals are very ambitious and not currently achievable by the O₂ measurement 405 community; hence the “extended” O₂ goals, which are suitable for some O₂ applications, shown in parenthesis.

The repeatability is determined from the mean $\pm 1\sigma$ standard deviations of the average of two consecutive measurements of the TT. For the G2207-*i* this is equal to $\pm 5.69 \pm 5.61$ per meg, compared to $\pm 2.21 \pm 1.96$ per meg on the Oxzilla. Previous to applying the RT interpolation to the G2207-*i* data, the repeatability of the G2207-*i* was $\pm 11.86 \pm 13.83$ per meg, twice as bad 410 as after the RT application; this is because after the RT interpolation was applied the large jumps in the TT value after a WSS calibration were removed. In the context of the WMO repeatability goals, neither the Oxzilla nor the G2207-*i* meet the goal of ± 1 per meg. For O₂, the WMO the goals are very ambitious and not currently achievable by the O₂ measurement community; hence, the “extended” O₂ repeatability goal of ± 5 per meg (Crotwell et al., 2019). The Oxzilla TT results lie within this 415 extended goal, however the G2207-*i* does not, even after the application of the RT, meaning that the G2207-*i* is not considered precise enough within the WMO goals, although it is close.

The compatibility of the analyser, which ~~provides a measure of the compatibility to the SIO O₂-scale over time, and~~ is here used as a proxy for accuracy, is determined by calculating the mean difference between the TT O₂ as measured by the G2207-*i* and the VUV declared value (-718 per meg). The mean absolute difference from the declared value on the VUV for the Oxzilla is 3.03 ± 2.59 per meg, this is well within the extended WMO compatibility goal of ± 10 per meg and is quite close to 420 more stringent goal of ± 2 per meg. The compatibility of the G2207-*i* prior to the application of the RT is 22.88 ± 34.11 per meg, which is far greater than even the extended compatibility goal of ± 10 per meg. After the application of the RT interpolation the compatibility of the G2207-*i* O_{2,NC} was calculated as 9.97 ± 6.71 per meg, although this is not within the WMO compatibility goal, it is just within the extended goal, which is deemed suitable for some applications in specific 425 circumstances, such as where the signals are very large as such that reduced repeatability and compatibility does not preclude useful information from the measurements.

The compatibility and repeatability of the G2207-*i* measurements were vastly improved after the application of a 5 hourly RT, however if ignoring the TT results immediately after a new WSS calibration (i.e., after the large jumps when the RT was not

430 applied) the repeatability without the RT interpolation is 5.21 ± 4.50 per meg, improving to 4.27 ± 4.61 per meg when the RT is applied. This is because the RT corrected for baseline drift between WSS calibrations, as the O_2 value of the WSSes was defined as a difference from the RT, but it does not correct for drift within the calibration period. However, as the TT results are imprecise (as illustrated by the large error bars in Fig. 8) even if any baseline drift within a calibration period were corrected for there would likely be little improvement in the final TT results as the noise in the RT corrected TT values is primarily caused by imprecision rather than baseline drift.

3.5 Applications of the G2207-*i* O_2 measurements in the calculation of fossil fuel CO_2

435 In order to further assess the G2207-*i*'s performance in real-world applications the fully dried, RT corrected, $O_{2,NC}$ observations from WAO were used to isolate the fossil fuel component of the concurrent CO_2 observations and then compared to the ff CO_2 values calculated from APO derived from the Oxzilla O_2 observations following the methodology outlined in Pickers et al. (2022). The resultant ff CO_2 values calculated from each analyser are displayed in Fig. 9, negative ff CO_2 values occur when the O_2 observations are above (more positive) than the calculated baseline.

440 The measurement uncertainty was calculated as the average hourly SD on 30 October 2019, this date was chosen as it was a particularly stable period with little variation in the TT results for both analysers (Fig. 8); the resultant uncertainty for the G2207-*i* is ± 11.19 per meg compared to ± 4.86 per meg for the Oxzilla. The uncertainty in the baseline ($\pm 28\%$), and the emission ratio uncertainty ($\pm 22\%$) are significantly larger than these measurement uncertainties (Pickers et al., 2022), but as these are the same for both analysers the additional measurement uncertainty for the G2207-*i* caused by analyser noise increases the uncertainty of the calculated ff CO_2 values. The average final calculated uncertainty on the ff CO_2 values calculated from the Oxzilla measurements is 5.82 ppm, compared to 12.97 ppm on the G2207-*i*.

450 The average ff CO_2 value over the entire full drying period for the Oxzilla is 5.06 ppm, compared to 7.86 ppm on the G2207-*i* (Table 4); the calculated ff CO_2 from the G2207-*i* is higher than that of the Oxzilla 73 % of the time. This difference is predominantly due to the higher O_2 values reported by the G2207-*i* as discussed in section 3.3.2; some of this difference also comes from the jumps in the G2207-*i* O_2 values which mean that the calculated baselines used for each analyser follow different trends (Fig. A1). For example, on the 27 October 2019 and 30 October 2019 the largest difference between the calculated ff CO_2 values is observed (Fig. 9), on both of these dates there is a large jump in O_2 values from the previous day measured by the G2207-*i* following a WSS calibration (Fig. 7). Although the O_2 difference between the two analysers on these days are low, there was a large difference the preceding day, the days with the larger difference (due to a higher O_2 value reported by the G2207-*i*) in observed values pull the baseline to become more positive, thus making the difference between the ff CO_2 calculated from the two analysers larger on days where the observed O_2 difference is smaller.

455 Although the G2207-*i* calculated ff CO_2 values are often higher than those from the Oxzilla, it still follows the same trend (with some jumps in the G2207-*i* values) however, the maximum and minimum values occur at different times. The differences in ff CO_2 calculated from the G2207-*i* and the Oxzilla will become problematic if using the G2207-*i* analyser for top-down ff CO_2 quantification on an hourly basis.

460 Formatted: Font: Not Italic

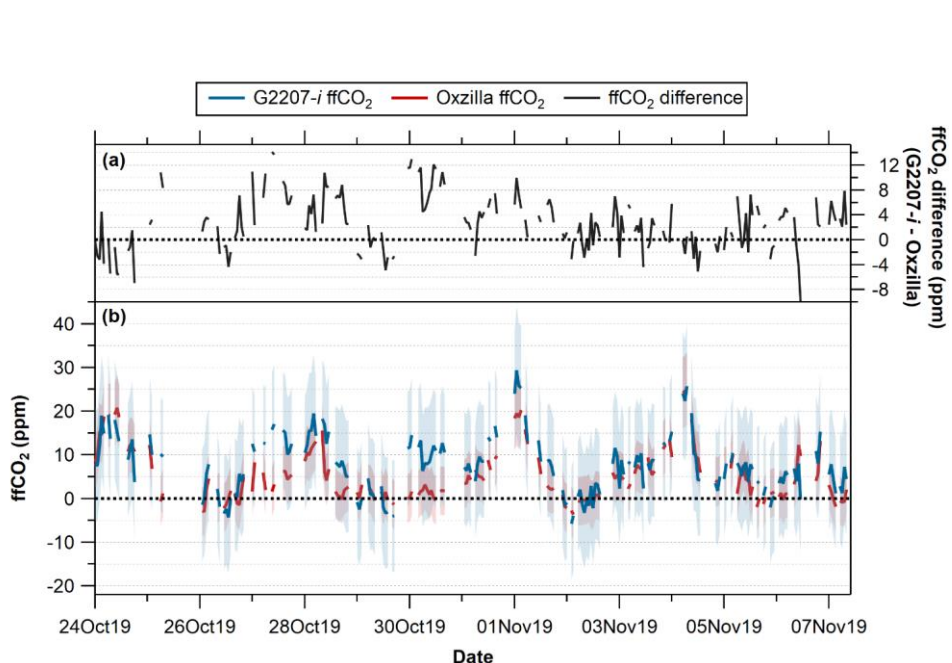


Figure 9. (a) Calculated ffCO₂ from the G2207-*i* and the Oxzilla, shaded areas indicate uncertainty of the calculated ffCO₂. (b) Difference between the ffCO₂ calculated using the G2207-*i* and the Oxzilla O₂ (G2207-*i* – Oxzilla). Dashed black lines indicates 0 ppm. N.B. Gaps are due to threshold requirement of a minimum of 20 minutes of data for hourly averages.

465

Table 4. Comparison of ffCO₂ values calculated from the Oxzilla and G2207-*i* O₂ measurements. Average values given $\pm 1\sigma$ standard deviation.

	Oxzilla ffCO ₂ (ppm)	G2207- <i>i</i> ffCO ₂ (ppm)
Average	5.06 ± 5.87	7.86 ± 6.63
Maximum	25.21	29.40
Minimum	-3.71	-6.47

4. Conclusions

The performance of the Picarro G2207-*i* under both laboratory and field conditions has been thoroughly evaluated. When

470 running a cylinder on the G2207-*i* over 24 hours in the laboratory, we observed a large amount of noise in the raw 1 second data, resulting in a large standard deviation in averaged data. This standard deviation is reduced over longer averaging time s.

During the laboratory measurement of cylinder gases with declared O₂ values, the G2207-*i* performed within the WMO

extended compatibility goal of ± 10 per meg when measuring cylinders with a negative O₂ per meg value. When measuring cylinders with a positive O₂ value, the precision and accuracy of the result worsened, thus the G2207-*i* is not recommended 475 for use in this range.

When sampling ambient air, we found that the G2207-*i*'s built-in water correction does not, at present, sufficiently correct for the influence of water vapour even when the sample air is partially dried, and therefore recommend full drying (<1 ppm H₂O) of air samples. When sampling fully dried air, large step-changes in the reported O₂ values from the G2207-*i* were observed after each WSS calibration; the addition of a RT every 5-hours vastly reduced these jumps however they were still observable.

480 When the RT routine was applied the repeatability of the G2207-*i* was $\pm 5.69 \pm 5.61$ per meg, falling just outside of the WMO extended goal of ± 5 per meg, it is possible that with a more frequent RT routine this repeatability will improve. The compatibility was $\pm 9.97 \pm 6.71$ per meg, falling within the WMO extended compatibility goal for O₂ of ± 10 per meg. In the future, investigation into increased frequency of the running of a RT to reduce jumps in the observed O₂ values after a WSS calibration may improve both the repeatability and compatibility of the analyser. A key benefit of CRDS analysers is that they 485 do not require drying of the air sample and consume considerably less gas than current methods, however, this is not currently the case with the G2207-*i* for O₂ measurements.

Data Availability.

490 The G2207-*i* data from WAO and CRAM HLab tests are available at <https://doi.org/10.5281/zenodo.6802657> (Fleming et al., 2022)

The WAO O₂ and CO₂ in situ datasets are available from the CEDA data archives, which can be found at:

<https://catalogue.ceda.ac.uk/uuid/36517548500e1e4e85c97d99457e268a> (Weybourne Atmospheric Observatory et al., 2006)

Author contributions.

495 LSF, ACM, and PAP developed the measurement methodology, which while the measurements were conducted by LSF at UEA and WAO. AJE developed the software used to run the analyser. Investigation and visualisation were completed by LSF.

Writing was completed carried out by LSF. Review and editing were completed done by LSF, ACM, PAP and GLF.

Competing interests.

The authors declare that they have no conflict of interest.

Acknowledgements.

500 We are very grateful to M. Hewitt, N. Griffin, and D. Blomfield (UEA) for supporting the WAO measurements. We are also very grateful to G. Lucic and M. Hoffmann at Picarro Inc. for the loaning of the G2207-*i* analyser and their feedback on the a draft manuscript. LSF is supported by the UK Natural Environment Research Council (NERC) "EnvEast" Doctoral Training Partnership, grant number NE/L002582/1. The WAO atmospheric O₂ and CO₂ measurements are supported by the Atmospheric Measurement and Observation Facility (AMOF) of the National Centre for Atmospheric Science (NCAS), in addition to NERC research grants NE/R011532/1, [NE/N016238/4](https://doi.org/10.5281/zenodo.6802657), NE/S004521/1.

References

Battle, M. O., Munger, J. W., Conley, M., Sofen, E., Perry, R., Hart, R., Davis, Z., Scheckman, J., Woogerd, J., Graeter, K., Seekins, S., David, S., and Carpenter, J.: Atmospheric measurements of the terrestrial O₂ : CO₂ exchange ratio of a midlatitude forest, *Atmos. Chem. Phys.*, 19, 8687-8701, <https://doi.org/10.5194/acp-19-8687-2019>, 2019.

510 Bender, M. L., Tans, P. P., Ellis, J. T., Orchardo, J., and Habfast, K.: A high precision isotope ratio mass spectrometry method for measuring the O₂/N₂ ratio of air, *Geochimica et Cosmochimica Acta*, 58, 4751-4758, [https://doi.org/10.1016/0016-7037\(94\)90205-4](https://doi.org/10.1016/0016-7037(94)90205-4), 1994.

Berhanu, T. A., Hoffnagle, J., Rella, C., Kimhak, D., Nyfeler, P., and Leuenberger, M.: High-precision atmospheric oxygen measurement comparisons between a newly built CRDS analyzer and existing measurement techniques, *Atmos. Meas. Tech.*, 12, 6803-6826, <https://doi.org/10.5194/amt-12-6803-2019>, 2019.

Blaine, T. W., Keeling, R. F., and Paplawsky, W. J.: An improved inlet for precisely measuring the atmospheric Ar/N₂ ratio, *Atmos. Chem. Phys.*, 6, 1181-1184, <https://doi.org/10.5194/acp-6-1181-2006>, 2006.

520 Chen, H., Winderlich, J., Gerbig, C., Hoefer, A., Rella, C. W., Crosson, E. R., Van Pelt, A. D., Steinbach, J., Kolle, O., Beck, V., Daube, B. C., Gottlieb, E. W., Chow, V. Y., Santoni, G. W., and Wofsy, S. C.: High-accuracy continuous airborne measurements of greenhouse gases (CO₂ and CH₄) using the cavity ring-down spectroscopy (CRDS) technique, *Atmos. Meas. Tech.*, 3, 375-386, <https://doi.org/10.5194/amt-3-375-2010>, 2010.

Crotwell, A., Lee, H., and Steinbacher, M.: Report of the 20th WMO/IAEA Meeting on Carbon Dioxide, Other Greenhouse Gases and Related Measurement Techniques (GGMT-2019), World Meteorological Organization Global Atmospheric Watch, 525 Jeju Island, South Korea Report Series #255, 2019.

Dlugokencky, E. J. and Tans, P. P.: Trends in Atmospheric Carbon Dioxide. National Oceanic and Atmospheric Administration, Earth System Research Laboratory (NOAA/ESRL), https://gml.noaa.gov/ccgg/trends/gl_gr.html, last access: 17 Oct 2022, 2022.

530 Fleming, L. S., Manning, A. C., Pickers, P. A., Forster, G. L., and Etchells, A. J.: Datasets for "Evaluating the performance of a Picarro G2207-i analyser for high-precision atmospheric O₂ measurements" [dataset], <https://doi.org/10.5281/zenodo.6802657>, 2022.

ICOS-RI: ICOS Atmosphere Station Specifications V2.0, ICOS ERIC, <https://doi.org/10.18160/GK28-2188>, 2020.

Keeling, R. F.: Measuring correlations between atmospheric oxygen and carbon-dioxide mole fractions - a preliminary study in urban air, *J. Atmos. Chem.*, 7, 153-176, <https://doi.org/10.1007/bf00048044>, 1988a.

535 Keeling, R. F.: Development of an Interferometric Oxygen Analyzer for Precise Measurement of the Atmospheric O₂ Mole Fraction, UMI, 1988b.

Keeling, R. F. and Manning, A. C.: 5.15 - Studies of Recent Changes in Atmospheric O₂ Content, in: *Treatise on Geochemistry* (Second Edition), edited by: Holland, H. D., and Turekian, K. K., Elsevier, Oxford, 385-404; doi: <https://doi.org/10.1016/B1978-1010-1008-095975-095977.000420-095974>, <https://doi.org/10.1016/B978-0-08-095975-7.00420-4>, 2014.

Keeling, R. F. and Shertz, S. R.: Seasonal and interannual variations in atmospheric oxygen and implications for the global carbon cycle, *Nature*, 358, 723-727, <https://doi.org/10.1038/358723a0>, 1992.

Keeling, R. F., Manning, A. C., McEvoy, E. M., and Shertz, S. R.: Methods for measuring changes in atmospheric O₂ concentration and their application in southern hemisphere air, *Journal of Geophysical Research: Atmospheres*, 103, 3381-3397, <https://doi.org/10.1029/97JD02537>, 1998.

545 Keeling, R. F., Manning, A. C., Paplawsky, W. J., and Cox, A. C.: On the long-term stability of reference gases for atmospheric O₂/N₂ and CO₂ measurements, *Tellus B*, 59, 3-14, <https://doi.org/10.1111/j.1600-0889.2006.00228.x>, 2007.

Kozlova, E. A. and Manning, A. C.: Methodology and calibration for continuous measurements of biogeochemical trace gas and O₂ concentrations from a 300-m tall tower in central Siberia, *Atmos. Meas. Tech.*, 2, 205-220, <https://doi.org/10.5194/amt-2-205-2009>, 2009.

550 Manning, A. C.: Temporal variability of atmospheric oxygen from both continuous measurements and a flask sampling network: Tools for studying the global carbon cycle, Ph.D., Scripps Institution of Oceanography, University of California, San Diego, La Jolla, California, U.S.A., 202 pp., 2001.

Manning, A. C., Keeling, R. F., and Severinghaus, J. P.: Precise atmospheric oxygen measurements with a paramagnetic oxygen analyzer, *Glob. Biogeochem. Cycle*, 13, 1107-1115, <https://doi.org/10.1029/1999GB900054>, 1999.

Pickers, P. A.: New applications of continuous atmospheric O₂ measurements: Meridional transects across the Atlantic Ocean, and improved quantification of fossil fuel-derived CO₂, School of Environmental Sciences, University of East Anglia, Norwich, UK, 262 pp., 2016.

560 Pickers, P. A., Manning, A. C., Sturges, W. T., Le Quéré, C., Mikaloff Fletcher, S. E., Wilson, P. A., and Etchells, A. J.: In situ measurements of atmospheric O₂ and CO₂ reveal an unexpected O₂ signal over the tropical Atlantic Ocean, *Glob. Biogeochem. Cycle*, <https://doi.org/10.1002/2017GB005631>, 2017.

Pickers, P. A., Manning, A. C., Quéré, C. L., Forster, G. L., Luijkh, I. T., Gerbig, C., Fleming, L. S., and Sturges, W. T.: Novel quantification of regional fossil fuel CO₂ reductions during COVID-19 lockdowns using atmospheric oxygen measurements, 8, eab19250, <https://doi.org/10.1126/sciadv.abl9250>, 2022.

565 Rella, C. W., Chen, H., Andrews, A. E., Filges, A., Gerbig, C., Hatakka, J., Karion, A., Miles, N. L., Richardson, S. J., Steinbacher, M., Sweeney, C., Wastine, B., and Zellweger, C.: High accuracy measurements of dry mole fractions of carbon dioxide and methane in humid air, *Atmos. Meas. Tech.*, 6, 837-860, <https://doi.org/10.5194/amt-6-837-2013>, 2013.

Resplandy, L., Keeling, R. F., Eddebar, Y., Brooks, M., Wang, R., Bopp, L., Long, M. C., Dunne, J. P., Koeve, W., and Oschlies, A.: Quantification of ocean heat uptake from changes in atmospheric O₂ and CO₂ composition, *Scientific Reports*, 9, 20244, <https://doi.org/10.1038/s41598-019-56490-z>, 2019.

570 Ruckstuhl, A. F., Henne, S., Reimann, S., Steinbacher, M., Vollmer, M. K., O'Doherty, S., Buchmann, B., and Hueglin, C.: Robust extraction of baseline signal of atmospheric trace species using local regression, *Atmos. Meas. Tech.*, 5, 2613-2624, <https://doi.org/10.5194/amt-5-2613-2012>, 2012.

Severinghaus, J. P.: Studies of the terrestrial O₂ and carbon cycles in sand dune gases and in biosphere 2, United States, <https://doi.org/10.2172/477735>, 1995.

Steinbach, J., Gerbig, C., Rodenbeck, C., Karstens, U., Minejima, C., and Mukai, H.: The CO₂ release and Oxygen uptake from Fossil Fuel Emission Estimate (COFFEE) dataset: effects from varying oxidative ratios, *Atmos. Chem. Phys.*, 11, 6855-6870, <https://doi.org/10.5194/acp-11-6855-2011>, 2011.

580 Stephens, B. B., Keeling, R. F., and Paplawsky, W. J.: Shipboard measurements of atmospheric oxygen using a vacuum-ultraviolet absorption technique, *Tellus B: Chemical and Physical Meteorology*, 55, 857-878, <https://doi.org/10.3402/tellusb.v55i4.16386>, 2011.

Stephens, B. B., Bakwin, P. S., Tans, P. P., Teclaw, R. M., and Baumann, D. D.: Application of a differential fuel-cell analyzer for measuring atmospheric oxygen variations, *Journal of Atmospheric and Oceanic Technology*, 24, 82-94, 10.1175/JTECH1959.1, 2007.

585 Stephens, B. B., Keeling, R. F., Heimann, M., Six, K. D., Murnane, R., and Caldeira, K.: Testing global ocean carbon cycle models using measurements of atmospheric O₂ and CO₂ concentration, *Glob. Biogeochem. Cycle*, 12, 213-230, <https://doi.org/10.1029/97GB03500>, 1998.

590 Tohjima, Y.: Method for measuring changes in the atmospheric O₂/N₂ ratio by a gas chromatograph equipped with a thermal conductivity detector, *Journal of Geophysical Research: Atmospheres*, 105, 14575-14584, <https://doi.org/10.1029/2000JD900057>, 2000.

Tohjima, Y., Mukai, H., Machida, T., Hoshina, Y., and Nakaoka, S. I.: Global carbon budgets estimated from atmospheric O₂/N₂ and CO₂ observations in the western Pacific region over a 15-year period, *Atmos. Chem. Phys.*, 19, 9269-9285, <https://doi.org/10.5194/acp-19-9269-2019>, 2019.

595 Tohjima, Y., Machida, T., Watai, T., Akama, I., Amari, T., and Moriwaki, Y.: Preparation of gravimetric standards for measurements of atmospheric oxygen and reevaluation of atmospheric oxygen concentration, *Journal of Geophysical Research: Atmospheres*, 110, <https://doi.org/10.1029/2004JD005595>, 2005.

Werle, P., Mücke, R., and Slemr, F.: The limits of signal averaging in atmospheric trace-gas monitoring by tunable diode-laser absorption spectroscopy (TDLAS), *Applied Physics B*, 57, 131-139, <https://doi.org/10.1007/BF00425997>, 1993.

600 Weybourne Atmospheric Observatory, Forster, G., and Bandy, B.: Weybourne Atmospheric Observatory (WAO): surface meteorology and atmospheric chemistry data [dataset], <http://catalogue.ceda.ac.uk/uuid/36517548500e1e4e85c97d99457e268a>, 2006.

Wilson, P. A.: Insight into the Carbon Cycle from Continuous Measurements of Oxygen and Carbon Dioxide at Weybourne Atmospheric Observatory, UK, School of Environmental Sciences, University of East Anglia, Norwich, UK, 2013.

605 Zhao, C. L. and Tans, P. P.: Estimating uncertainty of the WMO mole fraction scale for carbon dioxide in air, *Journal of Geophysical Research: Atmospheres*, 111, <https://doi.org/10.1029/2005JD006003>, 2006.